MEASUREMENT OF NOSE RADIUS AND WEAR OF MULTIPLE CUTTING TOOL INSERTS FROM 2-D SCANNED IMAGES WITH SUB-PIXEL EDGE DETECTION

LIM TEONG YEONG

UNIVERSITI SAINS MALAYSIA

2015

MEASUREMENT OF NOSE RADIUS AND WEAR OF MULTIPLE CUTTING TOOL INSERTS FROM 2-D SCANNED IMAGES WITH SUB-PIXEL EDGE DETECTION

by

LIM TEONG YEONG

Thesis submitted in fulfillment of the requirements
for the degree of
Doctor of Philosophy

March 2015

ACKNOWLEDGEMENTS

First of all, I would like to express my gratitude to my supervisor, Professor Dr. Mani Maran Ratnam, for his support and motivation throughout this research work. His guidance and incisive advice have inspired me to generate fruitful approaches in achieving the objectives in this research. Without his effort, I would not able to proceed and bring this research to a completion.

My heartfelt gratitude is extended to my beloved parents, Lim Kim Soo and Ng Ngoh Bit, brothers, sisters and relatives that support me unlimitedly all along without any hesitation. I truly treasure their encouragement and moral support throughout these years. Also, I dedicate my appreciation to my wife, Huey Juin, my lovely son, Jin Hong that gives me the spiritual strength along this study journey. May they always be blessed with the merits of triple gems. Also, I would like to thank my late father in law, Mr. P'ng Choo Heng for his guidance and prospective advice.

Last but not the least, my sincere thanks and regards to all teachers and the members of Penang Life Education Center for their unlimited support and hard work. Their helpful and insightful assistance in any form has brought my life journey to a higher level of wisdom and consciousness.

TABLE OF CONTENTS

LIST OF TABLES

LIST OF FIGURES

LIST OF ABBREVIATIONS

AISI	American Iron and Steel Institute
BL	Back Light
BUE	Build-up Edge
CCD	Charge Coupled Device
CD	Centroid Distance
CDF	Cumulative Distribution Function
CIS	Contact Image Sensor
CNC	Computer Numerical Control
DOV	Degree of Overlap
DPI	Dots Per Inch
FL	Front Light
GHz	Giga Hertz
ISO	International Standard Organization
LCL	Lower Confident Limit
LED	Light Emitting Diode
LOA	Limits of Agreement
ND	Neutral Density
OS	Operating System
PC	Personal Computer
RMSE	Root Mean Square Error
ROI	Region of Interest
SF	Scaling Factor
SSE	Sum of Square Error
TCMS	Tool Condition Monitoring System
TWI	Tool Wear Index
UCL	Upper Confident Limit

LIST OF SYMBOLS

A	Matrix with a row and b column
A_p	Projected nose wear area
a	Row number of matrix
B	Column vector with a entries
b	Column number of matrix
D	Diameter of pin gauge
D_i	Internal boundary points
$\bar{d}$	Arithmetic mean difference
E	Compensated error in unit mm
E_i	External boundary points
E_x	Average error (global x direction scanning)
Ex_{max}	Maximum error (global x direction scanning)
Ex_{min}	Minimum error (global x direction scanning)
Ey	Average error (global y direction scanning)
Ey_{max}	Maximum error (global y direction scanning)
Ey_{min}	Minimum error (global y direction scanning)
e_h	Reduction factor
F	The empirical cumulative distribution function
f	Feed rate of machining
G	Standard normal CDF
H_0	Null hypothesis
H_1	Alternative hypothesis
h	Height of the tilted insert
h_1	Gray level of background pixels
h_2	Gray level of foreground pixels
I_b	Background intensity
IFocus	*InfiniteFocus*
k	Coverage factor

k_p	Edge location
k_e	Edge contrast
l	Arithmetic mean of l_1 and l_2
l_1, l_2	Edge parameters
m	Data range considered for nose region detection
m_i	Moments of input data
N	Resolution in DPI
n	Order of polynomial function
n_o	Number of independent observations
n_p	Total number of pixels
O	Approximate circle center
P	First coordinate of the actual detected nose region
P_{r1}	First fraction of the edge location k_p
P_{r2}	Second faction of the edge location k_p
P'	Shifted P with angle θ_p
p	Polynomial function using least-squares estimation
p_i	Coefficient of nth order polynomial function
Q	Last coordinate of the actual detected nose region
Q_d	Repeatedly measurement of input quantity
Q'	Shifted Q with angle θ_p
q_j	Individual observed values
$\bar{q}$	the estimate of the quantity Q_d
R	Actual circle center
R_a	Average surface roughness
$R1$, $R2$,$R3$, $R4$	Sections of image
R'	Shifted R with angle θ_p
r	Nose radius
r_e	Nominal nose radius
r_{1i}	Projection radius of unworn insert
r_{2i}	Projection radius of worn insert
SD	Standard deviation
SF	Global scaling factor
SF_{avg}	Average global scaling factor

SF'	Local scaling factor
$S1$	First coordinate of the estimated nose region
$S1'$	Range of coordinates of $S1$
$S2$	Last coordinate of the estimated nose region
$S2'$	Range of coordinates of $S2$
s_d	Empirical standard deviation
s_p	Parameter solution for input moments
s^2	Experimental variance
$\hat{s}_d$	Standard error of standard deviation
t	Paired student's t statistic value
U	Uncertainty of measurement
U_{CD}	Uncertainty of calibrated centroid distance
U_{Ex}	Uncertainty of average error (global x direction scanning)
U_{Ey}	Uncertainty of average error (global y direction scanning)
U_x	Uncertainty of absolute error (global x direction scanning)
$U'x$	Uncertainty of absolute error (local x direction scanning)
U_y	Uncertainty of absolute error (global y direction scanning)
U'_y	Uncertainty of absolute error (local y direction scanning)
u	Standard uncertainty
VB	Average width of the flank wear land
VB_c	Nose flank wear
$VB_{c(max)}$	Maximum nose flank wear
w	Width of stopper
X	Column vector with b entries
Xi	Input quantity
x	X-coordinate
x_{abs}	Absolute error (global x direction scanning)
x_{max}	Maximum absolute error (global x direction scanning)
x_{min}	Minimum absolute error (global x direction scanning)
x_o	X-coordinate of circle center
x'_{abs}	Absolute error (local x direction scanning)
x'_{max}	Maximum absolute error (local x direction scanning)
x'_{min}	Minimum absolute error (local x direction scanning)

y	Y-coordinate
y_{abs}	Absolute error (global y direction scanning)
y_{max}	Maximum absolute error (global y direction scanning)
y_{min}	Minimum absolute error (global y direction scanning)
y_o	Y-coordinate of circle center
y'_{abs}	Absolute error (local y direction scanning)
y'_{max}	Maximum absolute error (local y direction scanning)
y'_{min}	Minimum absolute error (local y direction scanning)
θ_p	Angle of rotation for image alignment
θ_s	Tilt angle
θ_r	Rotational angle
Δr_{total}	Summation of radial difference
σ_p	Parameter solution for input moments
α	Significant value of statistical test

PENGUKURAN JEJARI DAN KEHAUSAN MUNCUNG BAGI BERBILANG MATA ALAT PEMOTONG MENGGUNAKAN IMEJ IMBASAN 2-D DENGAN PENGESANAN PINGGIR SUB-PIKSEL

ABSTRAK

Jejari muncung alat pemotong mempengaruhi kualiti permukaan bahan kerja siap, kestabilan pemesinan, input kuasa serta keadaan alat peomotong kerana interaksi langsung muncung alat pemotong dengan bahan kerja semasa pemesinan. Pendekatan konvensional untuk mengukur jejari muncung dengan menggunakan profil projektor dan mikroskop dari pengeluar alat pemotong memerlukan titik-titik yang dipilih secara manual daripada profil muncung. Ini menyebabkan pengukuran yang tidak tepat kerana pemilihan beberapa titik daripada sektor bulatan yang tidak sempurna dari tepi muncung. Pendekatan terbaru untuk mengukur jejari dan kehausan muncung bagi berbilang alat pemotong dengan menggunakan imej 2-D yang diimbas dengan alat pengimbas kos rendah and resolusi tinggi adalah dicadangkan. Penyiasatan tentang kesan keadaan pencahayaan pengimbas, orientasi dan lokasi alat pemotong serta resolusi pada ketepatan pengesanan pinggir sub-piksel telah dijalankan. Keputusan pengukuran menggunakan pendekatan pengimbas adalah dibandingkan dengan projektor profil dan sistem metrologi pembolehubah fokus 3-D (*Alicona InfiniteFocus*). Kaedah transformasi kutub-jejari digunakan untuk mengira luas unjuran kehausan, A_p dan kehausan maksimum muncung flank, $VB_{C\ (max)}$

sebelum dan selepas pemesinan dengan menggunakan imej pengimbas dan *InfiniteFocus*. Pengukuran jejari muncung pelbagai alat pemotong menghasilkan ralat purata kurang daripada 1%. Kaedah projektor profil digital memberi ralat pengukuran muncung yang tinggi sebanyak 11%. Untuk pengukuran luas unjuran kehausan dan muncung flank, sisihan maksimum antara kedua-dua kaedah pengukuran adalah sebanyak 6% dengan nilai yang lebih rendah didapati daripada imej imbasan disebabkan perbezaan resolusi di antara kaedah pengimejan. Oleh itu, pendekatan kos rendah dengan ketepatan tinggi yang dicadangkan dalam kajian ini membolehkan penilaian yang cepat dan tepat daripada pelbagai alat pemotong dan menyediakan satu penyelesaian baru untuk pemeriksaan muncung serta pengukuran kehausan.

MEASUREMENT OF NOSE RADIUS AND WEAR OF MULTIPLE CUTTING TOOL INSERTS FROM 2-D SCANNED IMAGES WITH SUB-PIXEL EDGE DETECTION

ABSTRACT

The nose radius of a cutting tool insert is known to affect the surface quality of the finished workpiece, machining stability, power input as well as the condition of the insert due to the direct interaction of the tool nose with the workpiece during machining. Conventional approaches for measuring the nose radius using profile projector and toolmaker's microscope require manually selected points from the nose profile which cause inaccurate measurement of nose radius since only a few points from the sector of an imperfect circle from the nose edge are selected. A novel approach for the measurement of nose radius and wear of multiple cutting inserts using 2-D images scanned using a high resolution low-cost flatbed scanner is proposed. Investigation on the effect of scanner's lighting conditions, tool orientation and location on the accuracy of sub-pixel edge detection of nose radii were carried out. The results of the measurement of nose radii using the scanner approach were compared with a profile projector and the variable-focus 3-D metrology system (*Alicona InfiniteFocus*). The polar-radius transformation method was used to calculate the projected wear area, A_p and maximum nose flank wear, $VB_{c(max)}$ before and after machining using images from scanner and *InfiniteFocus*. The measurement of the nose radii of multiple inserts yielded average error of less than 1%. The digital

profile projector method yielded a highest error of about 11% in nose radii measurement. For the projected nose wear and nose flank measurement, the maximum deviation are about 6% with a slight underestimation of nose wear for scanner due to the resolution difference between the two scanning methods. Thus, the low-cost and high accuracy approach proposed in this study enables fast and accurate assessment of multiple tools and provides a new solution for tool nose inspection and wear measurement.

CHAPTER 1

INTRODUCTION

1.1 Background of Research

The surface finish quality and dimensional accuracy of a machined part plays a significant role in ensuring the quality and characteristics of the part, such as its tribological properties, fatigue strength and corrosion resistance (Kohli and Dixit, 2005). Some of the factors that affect the surface quality and dimensional accuracy of the finished part are the material hardness, cutting edge geometry, tool wear characteristics and machining conditions (Ozel *et al.*, 2005). Of particular significance in affecting the product quality is the tool geometry, especially the nose radius. Large nose radius results in deeper subsurface structural changes due to high plowing forces (Thiele and Melkote, 1999). In addition, the wear that occurs on the tool nose area, which is a combination of flank wear and notch wear (Jurkovic *et al.*, 2005; Stephenson and Agapiou, 1997), is also one of the major factors that affect the surface quality of work piece in turning operation (Kwon and Fischer, 2003).

Cutting tool inserts used for metal removal in machine tools are designed with various geometries. The tool nose radius of a cutting insert at the rounded tip of a single-point tool is known to affect the surface quality of the finished work piece, machining stability, heat generation, residual stress as well as the condition of the insert due to the direct interaction of the tool nose with the work piece during machining (Chou and Song, 2004; Liu *et al*., 2004; Campocasso *et al*., 2014; Adibi-

Sedeh *et al*., 2002). In theory, the idealized model of the average surface roughness of the work piece machined using a tool with a rounded nose is given by (Boothroyd 1988):

$$R_a = \frac{0.0321 f^2}{r_\varepsilon} \tag{1.1}$$

where r_ε is the nose radius and *f* is the feed rate. Thus, the tool nose radius and the feed rate have the greatest impact in determining the surface roughness. In practice, other factors such as the machining speed, depth-of-cut, material of tools and work piece also influence the surface integrity. According to Chou and Song (2004), the change of distance from the cutting edge to the nominal machined surface is a strong function of nose radius. A larger nose radius improves the surface finish. Shallow thread surface occurs whenever a tool having a small radius is used in conjunction with a large feed (Datsko, 1997). Conventionally, the recommended guidelines for nose radius are provided by the tool manufacturers based on the theoretical surface finish derived from Equation (1.1).

The nose radius is essentially the most vital tool geometry in Computer Numerical Control (CNC) machining. Acquiring the value of tool nose radius accurately is necessary because tool nose radius will cause deviations in the work piece dimensions due to overcutting or undercutting especially when tapers or free-form surfaces are to be machined (Zhou *et al*., 2009) as shown in Figure 1.1. The dimensional deviation affects the flatness, straightness, circularity, cylindricity, parallelism, perpendicularity, angularity and concentricity of machine products (Dotson *et al.*, 2003). The nose radius is also an important parameter for programming the tool path in CNC machine tools using nose radius compensation to

assure the dimensional accuracy of the finished part (Chai *et al*., 1996). Using the nose radius compensation based on the measured nose radius, the CNC system is expected to determine the offset direction in the programmable path. Thus, the accurate measurement of radius becomes prominent in industry especially when involving micro-machining of CNC (Zhou *et al*., 2009) and it is a must to measure the nose radius to micron scale to turn the micro parts with the right compensation model (Hanson, 2012).

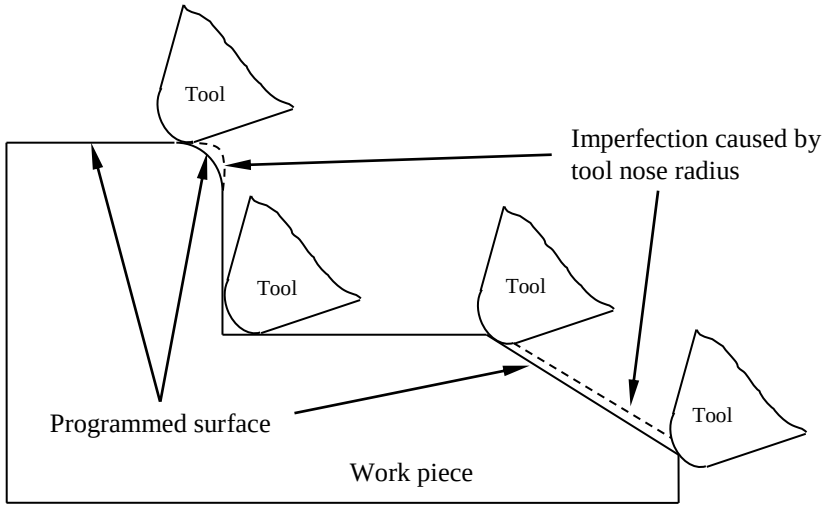

Figure 1.1. Deviations caused by the tool nose radius (Zhou *et al.* 2009).

The determination of nose radius is normally carried out using conventional measurement methods such as tool maker's microscope and profile projector (Chian and Ratnam, 2011). However, due to the large tolerance in the nose radius (±10% of nominal radius) allowed by the ISO 3685 standard (ISO 3685 International Standard, 1993), accurate measurement of the actual nose radius is a challenge. In the past, the nominal values of the nose radius were used in studying of the effect of nose radius and other machining parameters on surface roughness (Palanisamy *et al.*, 2008;

Kassim *et al.*, 2004.; Choudry and Bartaryam, 2003). In the conventional measurement method, only a few discrete points on the nose edge were chosen for radius measurement and this contributed significant errors in the measurement. According to Hopp (1994), high uncertainties of center coordinates measurement were found in the circle fitting process using three points on the edge of an arc. In addition, with the points extracted for fitting from a sector subtending less than about 60°, the radius has a very large uncertainty. Moreover, the effect of non-circularity in the nose sector due to the large radius tolerance on the measurement accuracy has been neglected in the past.

The polar radius transformation method for the measurement of radii as proposed by Chian and Ratnam (2011) used all the pixels in the nose region in determining the nose radius. The polar radius plot of the nose radius from a newly unworn insert showed that the nose profile appears to deviate from a circular profile. In their work, however, the nose edge extraction was based at pixel level and thus the accuracy of the measurement is limited by the resolution of the Charge Coupled Device (CCD) camera. Furthermore, using a CCD camera to capture image of the tool nose mounted on the tool holder and to measure the nose radius will introduce error because the tool holder itself has a relief angle that makes the tool tilted. This can be observed from the overestimation of nose radii with 11% mean deviation for majority of the cutting inserts measured.

Apart from the nose radius, another factor that significantly influences the surface finish of the machined part is the tool wear. Tool wear is usually the most relevant parameter inspected in machining because is has direct influence on the final

product quality, the machine tool performance and the tool lifetime (Schmitt *et al*., 2012). The tool wear, specifically the nose wear, is one of the critical wear regions in determining the surface quality because it shortens the cutting tools and increases gradually the dimension of machined surface, thus introducing significant dimensional errors which could reach 0.03 mm - 0.05 mm (Marinov, 2005). In machining, there are basically three wear zones of a cutting insert according to its principal location on a cutting tool which are crater wear, flank wear and nose wear as illustrated in Figure 1.2. The nose wear, which generally consist of many combinations of wear along the nose edge, is the most noticeable type of wear that occurs because of the direct interaction of the tool nose with the machined parts as well as the chips formed during machining.

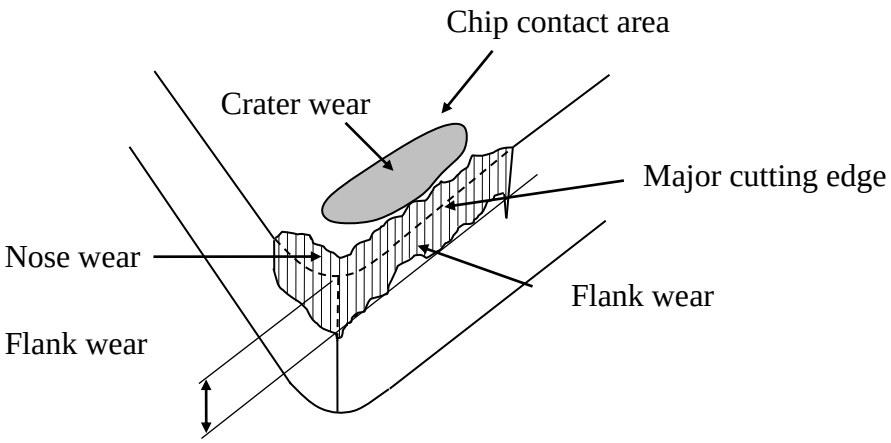

Figure 1.2. Typical cutting tool wear.

To monitor tool wear, intelligent tool condition monitoring systems (TCMS) have evolved rapidly using various sensor technology and instruments for monitoring, which include acoustic emission, tool temperature monitoring, force meter, accelerometer and other methods such as ultrasonic, optical measurements, work piece surface finish quality and dimensions measurement, stress/strain analysis and

spindle motor current (Snr and Dimla, 2000). However, many researchers have shown great interest in using machine vision as a direct non-contact way for assessing tool condition because machine vision has the advantage of (i) direct assessment of tool condition, (ii) micrometer scale measurement with high resolution image capture, (iii) examination and monitoring of wear patterns at different machining stages and (iv) archiving the images for future reference.

Machine vision using CCD camera was attempted in the past as an alternative to the conventional methods to measure nose radius and nose wear, where the cutting inserts were inspected using the digitized images (Shahabi and Ratnam 2008; Shahabi and Ratnam, 2009a; Shahabi and Ratnam, 2009b; Shahabi and Ratnam, 2010). Although CCD camera allows tool nose wear to be determined without removing the insert from the tool holder, the system is only capable of measuring single nose tip at a time with the aid of external lighting. However, machine vision system using CCD camera requires additional external lighting in obtaining the image. This requires the optimum adjustment of illumination angle, lighting intensity as well as to take into account the effect of ambient lighting. Thus, the images captured from a CCD camera will suffer from non-uniform illumination if any of these aspects were not properly considered. Besides that, CCD camera has limited field-of-view due to high magnification that allows only a single tool to be inspected at a time as well as optical distortions that requires periodic calibration whenever the experimental setup has been altered. Due to these problems, the use of a high resolution flatbed scanner is proposed in this work to acquire the images of the nose area for the measurement of nose radius, projected nose wear and nose flank wear, VB_c. Flatbed scanner has numerous advantages, such as (i) large field-of-view

compared to other system and hence allows the inspection of multiple tools, (ii) uniform illumination with built-in lighting, (iii) scanning of multiple regions of interest (ROIs) in one scan and (iv) high resolution with selectable resolution, and (v) low cost with convenient placement of multiple inserts. Using the scanner, the assessment of tool nose can be carried out in batches, thus allowing many tool inserts to be inspected in one scanning to decrease inspection time.

Current development of nose wear measurement using CCD camera is only up to one pixel level. For instance, Shahabi and Ratnam (2008) determined the nose wear by counting the number of pixels from the resultant image subtraction of the original and the machined tool nose. In another similar work (Shahabi and Ratnam, 2009b), the authors studied the nose radius wear from work piece roughness profile and compared the measurement using toolmaker's microscope.

Since the measurement of nose radii and the nose wear is an important precursor in precision machining and product quality control, the solution for fast and accurate assessment of these quantities are yet to be proposed. Although researchers in the past show great effort in assessing the nose conditions of the tool, there are aspects that have been overlooked which are (i) the use of nominal radius as the actual radius value in the published literature although it is known that the nominal radius has large tolerance, (ii) the use of conventional methods such as profile projector or microscope in measurement where the measurement obtained was considered the actual value in comparison to their method proposed and (iii) measurement was generally carried out one-at-a-time due to the small field of view of image acquisition device when digitizing the tool.

Due to the limitation of the existing methods in nose radius and nose wear measurement, the potential of the flatbed scanner as an image acquisition device for the measurement of nose radii and nose wear of multiple inserts was studied in this research work. The primary advantage of this method is that the whole image of cutting tool inserts can be captured and multiple edges can be processed and characterized in a single scanning process. Furthermore, many cutting tool inserts can be inspected in one batch of single image scanning that will indirectly save the inspection lead time. In the following sections, the main problems of the existing methods in nose radii and nose wear measurement are addressed in detail. Then, the research objectives and scopes are defined followed by a brief discussion of the current research approaches. The thesis outline is presented at the end of the chapter.

1.2 Problem Statement

Despite the important role of tool nose radius in machining, very few researchers have proposed a solution for the accurate measurement of the nose radius. To date, the best methods of measuring the nose radius of a cutting tool are either by using a tool maker's microscope that has automatic functions to determine radius from a selected number of points on the surface or by using a high-magnification profile projector. These methods require manually selected points from the nose profile which causes inaccurate measurement of nose radius since only a few points from the sector of a circle from the nose edge are selected. The main limitation of such methods is that the user has to manually select a number of points on the nose profile to determine the radius. Ideally, the nose radius measurement should be based on a large number of automatically selected points on the nose profile. But, this is not

possible if the measurement is performed manually. Since the manual points are selected visually, this also raises the question of whether accurate points are chosen for the nose radius estimation.

In addition, the tolerance of the nose radius specified by the manufacturer in accordance to ISO 3685 standard is ±10% of the nominal radius (ISO 3685, 1993). Since the profile of the tool nose may not be perfectly circular due to the ±10% tolerance allowed for nose radius in the standard, manual selection of a limited number of points on the nose profile for radius measurement will, at most, produce only an approximate value of the radius. Despite the large tolerance given by the manufacturer, the nominal radius is normally used by researchers in the study on the effect of nose radius on machining. With the shape of an unworn tool nose which is not a perfectly circular arc in nature, the accuracy of the relationships established between the studied parameters and the nose radius in most of the published literature are, therefore, ambiguous.

Machine vision system with a CCD camera has been proposed by researchers for measuring of nose radius as well as nose wear. However, image acquisition using a CCD camera has the disadvantages of providing a small field-of-view at high optical magnification and non-uniform illumination depending on the lighting. In the literature the measurement of nose radius and nose wear is generally carried out one insert at a time due to the small field-of-view of the image acquisition device, which is typically a CCD camera, used for digitizing the tool image. Past researchers have proposed nose radius and nose wear measurement by transforming the curved nose profile into a linear profile using polar-radius transformation. Although this is an

effective method for nose radius measurement, it is limited to individual insert measurement due to the limited field-of-view of the CCD camera. In all the other works reported in the literature the measurement of nose radius has been carried only on individual insert. Although multiple tool nose inspection provides convenience in terms of measurement time, it is not possible with the use of CCD camera or any other devices in image acquisition developed so far.

Recent developments of nose wear measurement using machine vision is only limited to pixel level accuracy. Despite the exhaustive efforts in measuring the nose wear using CCD camera, the proposed algorithms so far is only capable of giving the wear area to pixel level accuracy. The pixel-by-pixel subtraction of two images is at pixel-level accuracy and the edge pixels previously used in polar radius transformation were also at pixel level accuracy. However, for precise measurement of nose radius and nose wear, sub-pixel edges must be determined before the application of polar radius transformation. Hence, current methods of measuring nose radius and nose wear are still limited by the resolution of the imaging devices.

1.3 Research Objectives

The objectives of the research are as follows:

- To develop image processing algorithms for nose radius and nose wear measurement from the scanned images with sub-pixel accuracy using a high-resolution and a low-cost commercial flatbed scanner as an image acquisition device.

- To study the effect of scanner's lighting conditions, scanning resolutions, positions and orientation of tool placement on the accuracy of nose radii measurement of cutting tools from the scanned images.
- To develop image processing algorithms for multiple cutting tools scanning and measurement of nose radius and nose wear.
- To compare the accuracy of nose radius and nose wear measurement using the scanner method, optical profile projector and by processing images obtained from a commercial 3-D metrology system.

1.4 Research Scopes

This research is focused on the development of automatic tool nose radii and nose radius wear measurement using the scanned images from a common flatbed scanners. The research comprises calibration of scanner, selection of ideal lighting conditions, development of sub-pixel edge detection based on individual tool tips, accuracy study of nose radii measurement based on orientations and locations, batch measurement of nose radii and nose wear measurement. A localized sub-pixel edge detection algorithm is proposed in this research to locate the exact edge before the nose radius or nose radius wear can be measured. All measurement results obtained from the scanned images were compared with the measurement from the scanned images of *InfiniteFocus*. Uncertainty analysis was carried out to determine the accuracy of the measurement. For batch measurement of multiple inserts, only front lighting was used in scanning since the field of view of backlight condition is very small and cannot accommodate the scanning of batches of inserts whereas for *InfiniteFocus*, it only provides front light mode in scanning.

In this research, three geometrical types of cutting inserts (coated and uncoated) were used in the scanning namely triangular, rhombic and square. Each batch of scanning consists of several inserts with multiple tool tips from a particular type. Multiple tool inserts placed randomly on the glass platen of the scanner were detected and measured automatically.

1.5 Research Approach

A novel approach for the measurement of nose radius and wear of multiple cutting inserts using scanned 2-D images from a high resolution low-cost flatbed scanner is proposed. To obtain the high contrast and uniformly illuminated images from the scanner, an investigation of the effect of scanner's lighting conditions on the edge detection was carried out.

The measurement of tool nose is divided into nose radius measurement and nose radius wear measurement. For nose radius measurement, individual insert were first studied. The scanned images of individual inserts, which consists of the nose region and cutting edge, were subjected to image pre-processing and thresholding. The binary image was then morphologically eroded and dilated separately, and the inner and the outer boundary pixels that form the region of interest, were extracted from the eroded and dilated images. The maximum values of the first derivative of all the gray level profiles within the inner and the outer boundary pixels were determined to obtain the sub-pixel edge location. The nose profile was then determined geometrically and all the sub-pixel edge coordinates within the nose profile were subjected to radius estimation using circle fitting. The effect of tool

orientation on the accuracy of nose radii measurement was investigated by scanning the single tool placed at multiple orientations on the scanner's platen. In addition, the positional effects of a single tool on the accuracy of the nose radii measurement were also analyzed.

For batch measurement of nose radii from many inserts with multiple tool noses, the inserts were placed randomly and scanned. Algorithms to identify tool noses were developed and sub-pixel edge detection was applied to the cropped images of tool nose. In addition to this, the effect of resolution on radii measurement was also studied. The results of the measurement of nose radii using the scanner approach were compared with a digital profile projector and the commercial 3-D metrology system (Alicona *InfiniteFocus*) using statistical approach.

For the wear measurement the unworn insert before machining and the worn insert after machining were scanned separately. The sub-pixel edge detection developed was applied to both images and the images were realigned automatically to the same orientation. Then, the polar-radius transformation method was used to calculate the projected wear area. The nose flank wear (VB_c) was obtained from the tool geometry using the clearance angle of the cutting insert and the difference of nose radii of worn and unworn tool nose. Hence, the maximum of the nose flank wear ($VB_{c(max)}$) was determined. A similar measurement methodology was applied to images obtained from *InfiniteFocus* and was compared with the measurement of nose wear from scanning method.

For batch measurement of nose radius wear, the multiple inserts, each with multiple tool tips, was placed on the platen for scanning before and after machining. The scanned images was subjected to image pre-processing, thresholding, individual insert cropping, tool nose identification, auto-cropping of tool nose of the individual insert, sub-pixel edge detection and auto-realignment. Similarly, the polar-radius transformation method was used to calculate the projected wear area. Using the same approaches, measurement of nose wear of all inserts was conducted on the scanned images of cutting inserts before and after machining using *InfiniteFocus* and the comparison of measurement results were analyzed statistically.

1.6 Thesis Outline

This thesis is arranged in accordance to the scopes and objectives as mentioned above. Chapter 2 reviews the related work in nose radius and nose radius wear measurement and provides an overview of measurement methods from the published literature. A thorough discussion will be made to identify the advantages and limitations of existing approaches in assessing the nose radius and nose radius wear. Chapter 3 presents the methodology of the research in accordance to the scopes and objectives. Calibration of scanner, experimental setup, step-by-step development of computer algorithms for nose radius and nose radius wear measurement as well as the theory of accuracy for comparison of measurement approaches are detailed in this chapter. This is followed by the results and discussions in Chapter 4 which corresponds to each stage of experiments conducted. Subsequently, conclusions of this research are drawn in Chapter 5. Recommendations and suggestions are given for future work.

CHAPTER 2

LITERATURE REVIEW

2.1 Introduction

In this chapter, a review of current methods of measurement of tool nose radius and nose radius wear of cutting inserts will be made based on published literature. Three important components, namely, methods of nose radius and nose radius wear measurement, machine vision approaches in tool conditional monitoring and the background of flatbed scanner as an image acquisition tool in engineering measurement and its practical application in industry are reviewed in detail. Special attention will be given to the recent research interest in the precision measurement of nose radius and its wear conditions in accordance to ISO 3685 as well as to investigate the extent to which a commercially available high resolution scanner can be used as an effective image acquisition method in fine measurement.

2.2 Tool Nose Radius Measurement

The significant role of tool nose radius in machining and the current and conventional methods of measuring nose radius were reviewed in this section.

2.2.1 The Significant Role of Tool Nose Radius in Machining

Nose radius is a major factor that affects surface roughness of machined parts. A larger nose radius produces a smoother surface at lower feed rates and a higher

cutting speed. However, a larger nose radius reduces damping at higher cutting speeds, thereby contributing to a rougher surface (Dogra *et al*., 2011). Large nose radius tools have, along the whole cutting period, slightly better surface finish than small nose radius tools (Beauchamp *et al*., 1996; Kishawy and Elbestawi, 1997). Thus, a small radius is normally chosen for finishing or machining on thin and long workpiece whereas large radius is normally used in rough cutting in bigger diameter workpiece, where a strong cutting edge is needed. According to Chou and Song (2004), a large tool nose radius gives finer surface finish, decreased maximum uncut chip thickness and shallower white layers in new tool cutting, but the tool wear and specific cutting energy is slightly higher. The results are in agreement with the work published by Diniz and Micaroni (2002) where the authors concluded that to improve surface finish in dry condition, it is necessary to increase the tool nose radius and feed while decreasing the cutting speed. Similar results were obtained by Nath *et al*. (2009). The effect of tool nose radius on workpiece run-out (inaccuracy of rotating mechanical systems) and surface finish was further investigated by Shather (2009). A new relationship was found between nose radii and the run-out due to tool chatter that occurs during the machining of workpiece surface. Thus, nose radius is one of the most important geometrical factors governing the surface roughness criteria in machining.

Many researchers have attempted to investigate the relationship between tool nose radius and tool wear in the cutting performance. Generally, increasing the nose radius will increase the level of tool flank wear and cutting with a large nose radius results in a higher value of cutting forces due to the thrust force component (Thamma, 2008). Also, cutting with a small nose radius prolongs tool life, which was explained

by the reduction in the ploughing force. A study conducted by Endres and Kountanya (2002) shows the relationship between nose radius and flank wear on up-sharp and honed tools. The author observed that tool flank wear can be minimized for up-sharp tools by using a moderate nose radius whereas for tools with an edge radius, a wear-minimizing nose radius still exists but is higher than for up-sharp tools.

Despite the aforementioned conclusion, however, the proposed method used in the radius measurement has the disadvantage of getting the accurate estimation of radius because noisy images were obtained due to the effects of excessive grind marks. In addition to this problematic measurement, nose radius measurement was not part of the study interest where only the nominal radius sizes were employed. According to Liu *et al.* (2004), tool nose radius plays a significant role in deciding the shape of cutting cross-section in combination with depth of cut and feed rate whereby the chip morphology was related very strongly with nose radius. They concluded that the increase of tool nose radius leads to a remarkable increase of thrust force, residual tensile and compressive stress beneath the machined surface. Cassier *et al.* (2004) studied the built-up edge (BUE) phenomenon on the tool wear rate when turning at low cutting speed. The results obtained showed that when larger radius values are used, the largest values of flank wear were obtained which contradicts with the conventional results when high cutting speed is employed. Different types of steels (AISI 1020, AISI 1045, AISI 4140) and various machining parameters were studied, and the BUE effect was investigated. On the other hand, Thamizhmanii *et al.* (2007) showed that the formation of BUE formed as another cutting edge and thus increase the nose radius of the tool and produced a better surface at higher cutting speed. They also concluded that the worn out tool produced

better surface roughness than new tool initially because the cutting edge of the worn tool becomes un-uniformly larger nose radius which produced better surface finish. In contrary, if the amount of flank wear increases, a reduction in nose radius of the cutting tool occurs, this in turn reduces the surface finish of the product (Palanisamy *et al.*, 2008; Kassim *et al.*, 2004; Choudhury and Bartarya, 2003).

Despite the vital role of nose radius in machining, the nominal radius was presumed the true value in most of the published work although it is stated in ISO 3685 that a large tolerance of ±10% is allowed in the nose radius. Hence, the information of precise nose radius value was not obtained and the study of the correlation between the nose radius and the machining outputs on most of the published results (surface roughness, tool wear, residual stress and etc.) could lead to doubtful conclusion.

2.2.2 Measurement of Nose Radii

In precision engineering, tool nose radius compensation using geometric consideration of tool nose and the engagement conditions between the tool and work piece is normally introduced in CNC finish turning operation. This is because the tool nose is not an ideal circle and to some extent wear is expected after certain period of machining (Zhou *et al.*, 2009). Conventionally, the nose radius value was acquired using sample plates, caliper circular groove, tool microscope or a profile projector. These traditional methods of measurement allows fast and convenient results but at the same time incur errors due to two major problems: (i) tool nose is not perfectly circular (Chian and Ratnam, 2011), (ii) estimating of best circle using a few points from a sector of circle, which according to Hopp (1994), is highly

sensitive to errors in measurement when points extracted from a sector subtending less that 40° at the center are used for radius estimation. Due to the difficulty in obtaining the accurate nose radius, indirect measurement of tool nose in CNC turning was suggested by Zhou *et al.*(2009) using the tool parameters and the cutting geometry by radial error compensation. However, before the radial compensation takes place, the nose radius value of cutting insert was input to the numerical control lathe using microscope. In most of the traditional machining however, acquiring of nose radius is still relied on the conventional methods.

Blahusch *et al*. (1999) presented a method of measurements of tools using Halcon image processing tools with CCD camera. The outer boundary was extracted using sub-pixel edge detection and the radius was then approximated by lines and circular arcs. The use of back light condition in image capturing reduces the overexposure on the acquired image but at the same time causes light diffusion. This aspect was not taken into consideration in the image analysis when determining the nose radius. Chian and Ratnam (2011) proposed the measurement of tool nose radii of cutting inserts using machine vision. The curved nose profile was transformed into polar-radius plot and the determination of nose radius was based on the minimum average deviation of pixels from the straight line from the polar-radius plot. From their experiments, the nose radius was found to deviate from the nominal values. The best radius was defined based on the minimum deviation value from radius error plot. The method is very sensitive to alignment of the insert as the plane of the nose profile is required to be perpendicular to the optical axis of the CCD camera. Also, the measurement of radius was only up to one-pixel accuracy with only one single tool was measured at a time.

2.3 Tool Wear Measurement

The characteristics of tool wear according to ISO standard, methods of tool wear measurement as well as the machine vision approach to the tool wear assessment were reviewed in this section.

2.3.1 Characterization of Wear in Accordance to ISO 3685

Tool wear and tool failure are among the major problems in machining and have been studied extensively in the past in order to prevent inferior surface finish quality which may lead to scrap or re-work and in some cases causing damage to the machine tool itself (Kurada and Bradley, 1997a). The sensors for monitoring of tool wear include two major groups, which are direct sensors and indirect sensors (Kurada and Bradley, 1997b). The direct sensor measurement includes proximity sensors, radioactive sensors, and machine vision sensors, and the indirect sensing techniques include the cutting force signal monitoring, vibration signature analysis, cutting force analysis and acoustic monitoring system. In reality, the indirect methods require expensive and complex instrumentation setup which restricted its usage in a typical workshop and the signals could be influenced by other factors such as normal tool wear, machine vibration, and stress released during cutting (Shahabi and Ratnam, 2010) whilst the direct methods, such as machine vision system, requires less costly setup and are thus, conveniently implemented.

Generally there are three categories of tool wear in accordance to ISO 3685 (ISO 3685 International Standard, 1993), which are (i) wear of the major flank, (ii)

wear of the rake face and (iii) wear of the minor flank. The major flank wear is shown in Figure 2.1(a) and is the best known of tool wear. The growing width of the flank wear land leads to a reduction in the quality of the tool. The common criteria used for the assessment of flank wear is VB_{max} = 0.6 mm if the flank wear is not regularly worn, scratched, chipped or badly grooved in zone B; the average width of the flank wear land VB = 0.3 mm if the flank wear land is considered to be regularly worn in zone B. A combined wear of flank and the face wear forms the notch wear (Figure 2.1(a)) at the depth of cut line when the tool rubs against the shoulder of workpiece. Crater wear occurs at the rake face as a result of high thermal and shear stress due to the chip thickness as shown in Figure 2.1(b). The nose wear occurs mainly due to the abrasion wear mechanism of cutting tool's major edges resulting in an increase in negative rake angle where the nose edge deformed plastically at high speed machining (Figure 2.1(b)).

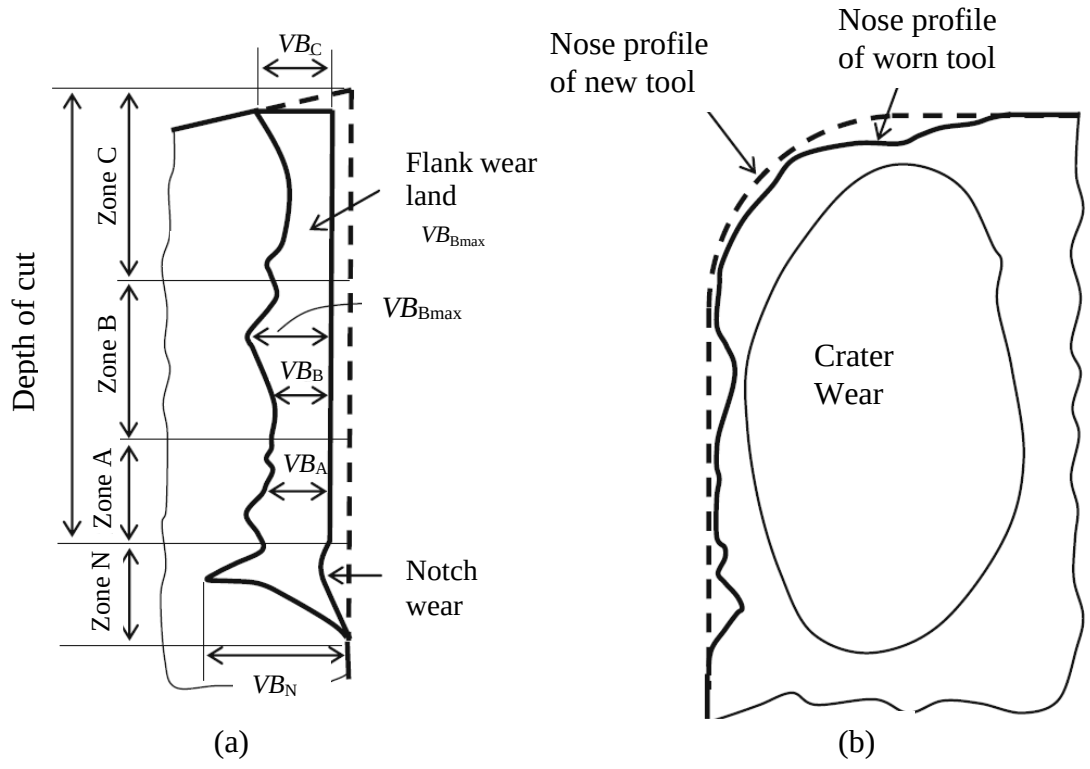

Figure 2.1. (a) Side view of insert showing flank wear (b) top view of insert showing nose profile and crater wear (ISO 3685 International standard, 1993).

According to ISO 3685, nose deformation will in most cases lead to a more rapid occurrence of catastrophic failure of high-speed steel tools and this makes the consequences of oxidation of carbide tools more severe. Other types of tool wear such as chipping, fracture, flaking, fatigue crack and breakage are shown in Figure 2.2.

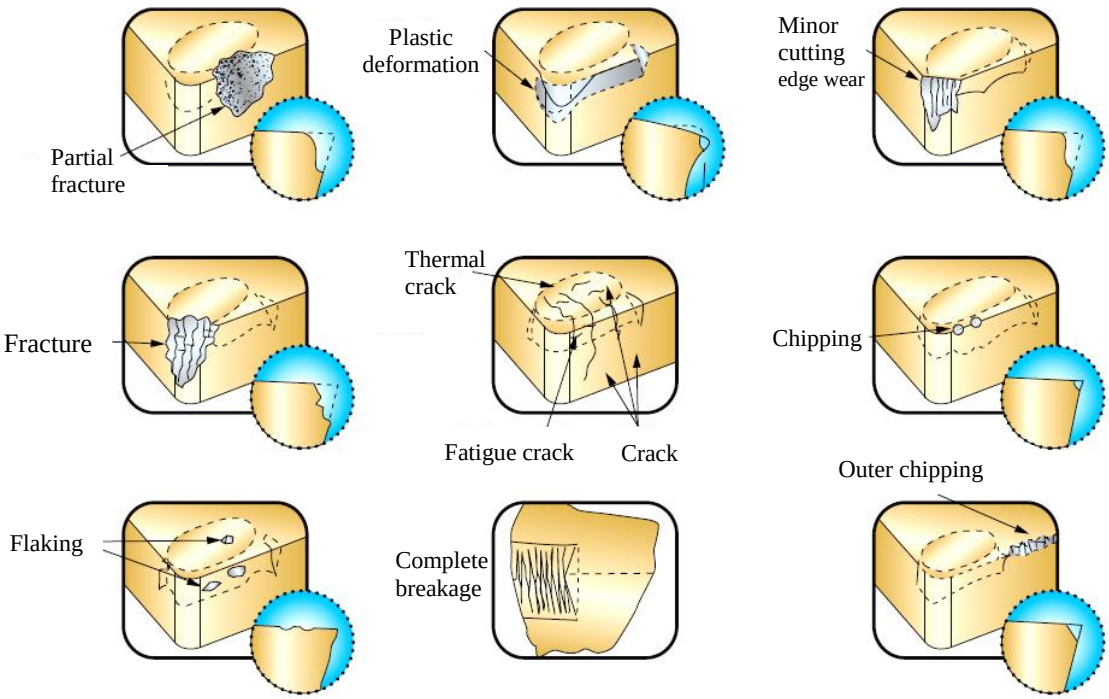

Figure 2.2. Some other types of tool wear in cutting tools (Sowa Tools and Machines Co. Ltd, 2010).

Amongst all the wear types, the nose wear, which generally consists many combinations of wears along the nose edge, is the most noticeable type of wear that occurs because of the direct interaction of the tool nose with the machined parts as well as the chips formed during machining. The deformation process during the machining is normally accompanied by the rubbing action with high friction that generates heat in plastic deformation. The nose area, which is located at the tool-chip interface and tool-work contact surface, is subjected most severe rubbing as shown in

Figure 2.3. Thus, the nose area wears down due lower strength and wear resistance when the temperature increases.

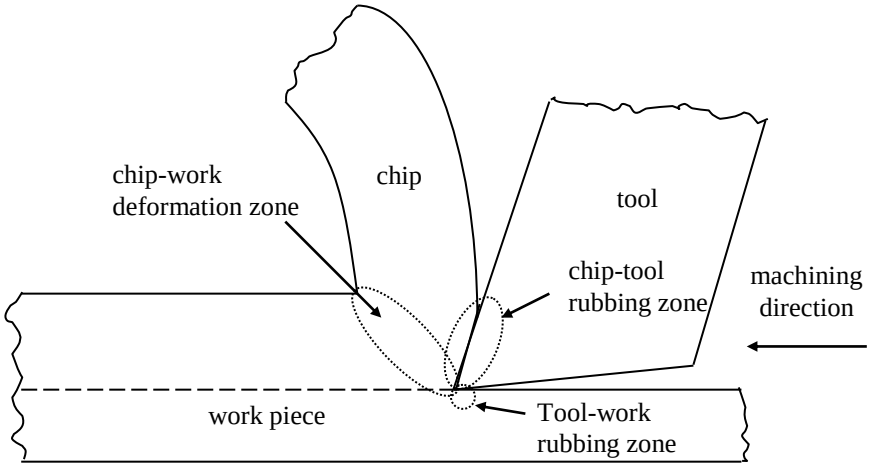

Figure 2.3. Heat producing zones in machining.

Although the nose wear is primarily important type of tool wear, and has a more profound effect on the surface roughness (Shahabi and Ratnam, 2009a), this category of wear is not well defined so far in any of the standards. Most of the past works on tool wear assessment focused on the measurement of flank wear (Wang *et al*., 2006; Kerr *et al*., 2006; Wang *et al*., 2005; Jurkovic *et al*., 2005)) and crater wear (Wang *et al*., 2006; Devillez *et al*., 2004) partly due to the tool life criteria defined in ISO 3685 standard. However, in ISO 3685 only the flank wear occurs at the zone C, VB_c was mentioned in accordance to its wear state at the nose edge. No further criterion was made about the allowable wear condition of nose in worn cutting tools. Recent research of interest on the assessment of nose wear was attempted by Shahabi and Ratnam (2008), Shahabi and Ratnam (2009a), Shahabi and Ratnam (2009b) and Mook *et al*. (2009) using machine vision system. Despite the efforts in determining the nose wear, the comparison of measurement results with tool's maker's microscopes showed comparatively large range of deviation between the two

measurements (Shahabi and Ratnam, 2009a). The limitation of the proposed method which required the nose profile to be perfectly circular in order to obtain the nose wear area (Mook *et al*., 2009) is practically impossible.

2.3.2 Nose Wear Measurement –Machine Vision Approach

In the development of automated tool wear measurement, machine vision approach has become more popular because they can be applied to assess tool wear directly through various stages of wear patterns analysis. Generally, a high resolution camera is used as an image acquisition tool to capture the image of the tool wear and enables micro-scale measurement with high magnification.

Various image processing and visualization methods have been published to characterize the appearance of tool wear using machine vision. Sortino (2003) proved that the conventional edge detection methods are not reliable solutions and thus implemented statistical filtering and high pass filtering. Due to the noisy detected edges, the measurement error is as high as 10% with a maximum error greater than 30%. In addition, using the high pixel width of 10 microns, the accuracy decreases drastically if the worn zone is very thin. Wang *et al*. (2005) presented a threshold independent method with sub-pixel accuracy to measure the flank wear area. An exhaustive windowing process was conducted using line-by-line pixel scanning and the highest accuracy was 8% by testing only on 10 samples with different insert types. In fact, the proposed algorithm necessitate the allocation of reference line and image realignment before the scanning process starts and thus affects the accuracy of subsequent processes. Despite the computationally intensive method developed, it was only applied to flank wear measurement.